Journal of Natural Gas Science and Engineering, Volume 36, Part A, November 2016, Pages 434–441
DOI:10.1016/j.jngse.2016.10.064

Liquid Loading in Gas Wells: Experimental Investigation of Back Pressure Effects on the Near-Wellbore Reservoir

Xiaolei Liu [a,*], Gioia Falcone [b], and Catalin Teodoriu [c]

[a] *Institute of Petroleum Engineering, University, Clausthal University of Technology, 38678, Clausthal-Zellerfeld, Germany*
[b] *Oil and Gas Engineering Centre, Cranfield University, MK43 0AL, Cranfield, UK*
[c] *Mewbourne School of Petroleum and Geological Engineering, The University of Oklahoma, 73019-1003, Oklahoma, USA*

Abstract A large-scale core-flooding experimental setup was designed and constructed to investigate the back pressure effects on transient flow through porous medium, and so mimic the physical process of liquid loading and reservoir response. Between initial and final steady-state flowing conditions, where inlet pressure was maintained at a constant level while initiating a transient pressure build up at the core sample end, an "U-shaped" temporal distribution of pore fluid pressure within the medium itself was observed, which is in direct contrast to the conventional reservoir pressure profile.

Keywords: Liquid loading; Gas wells; Core-flooding experiments; Back pressure

1. Introduction

In recent decades, considerable research has been conducted on liquid loading and many well established approaches have been used to alleviate its effects on gas production. However, the current methods for modelling/predicting liquid loading have oversimplified the role of transient phenomena in the near-wellbore reservoir.

After the onset of liquid loading, accumulated liquids at the bottomhole will create a back pressure, at a given instant, to restrict gas flow from the near wellbore region. Once the hydraulic head is equal to the reservoir pressure, the gas flow in the wellbore will cease. Considering these subsequent transient phenomena, liquid loading is a dynamic issue that involves both wellbore and reservoir. This research focused on experimental and numerical investigations of back pressure effects on transient flow through the near-wellbore reservoir.

In this study, the concept of the U-shaped pressure profile along the near-wellbore region of a reservoir under transient flow conditions was experimentally and numerically reproduced for single-phase gas flow in large-scale tests for the first time.

1.1 Liquid loading

In theory, every gas well will experience liquid loading in the latter stages of its producing life, becoming incapable of carrying liquids associated with produced gas to the surface. This leads to an increasing back pressure due to a rising liquid column at the bottomhole, which initially decreases deliverability, then prevents gas flow from reservoir, and eventually kills the well (Falcone and Barbosa Jr., 2013).

To identify associated subsequent dynamic behaviors in liquid loading, such as liquids accumulation and fluids re-injection, the relevant loading evolution over time must be investigated. The liquids accumulation process in loaded gas wells begins with the gas flow rate being greater than its critical flow rate, so all liquids in the tubing can be lifted to the surface by a gas core under steady state conditions (Coleman et al., 1991). With reservoir pressure depletion, the actual gas flow rate in the wellbore becomes less than the critical flow rate, causing liquids to holdup at the bottomhole. Once the hydraulic back pressure due to a column of accumulated liquids balances the reservoir pressure, the well will be completely loaded and the gas flow will decrease to zero.

* Corresponding author, E-mail address: xiaolei.liu@tu-clausthal.de (X. Liu).

To better understand reservoir behaviors in liquid loading, Zhang et al. (2010) developed a transient near-wellbore reservoir simulator based on a numerical 1-D, two-phase system code using an IMPES method to implicitly solve for pressures and explicitly solve for phase saturations. The authors stated that a "U-shaped" pressure profile can be generated along the near-wellbore region by reason of the pressure variation in the wellbore (Fig. 1). When the bottomhole pressure oscillates, the reservoir pressure response is not instantaneous and can even be particularly slow in low permeability formations due to a combination of inertia and compressibility effects. The "U-shaped" pressure profile could also explain the re-injection of the heavier phase into the reservoir. The bottomhole pressure oscillations acted as a boundary condition in this modeling effort.

One of the key objectives of this study was to verify the concept of the U-shaped pressure profile experimentally and numerically. Initially, to avoid the complexity of two-phase flow, single gas was used as the test fluid in our study.

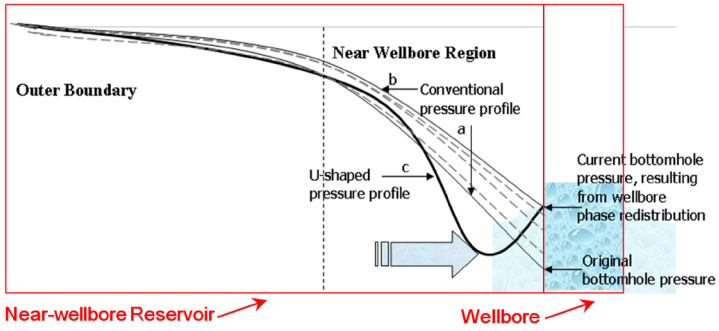

Fig. 1. Schematic of the "U-shaped" pressure profile generated by the transient reservoir simulator developed by Zhang et al. (2010).

Wang (2012) and Liu (2016) experimentally verified the U-shaped pressure concept through a small-scale core-flooding facility with single-phase compressible flows. A Hassler cell, which could accommodate a core sample of 30 cm length and 2.58 cm diameter, was modified to mimic the effect of varying downhole pressure on gas flows in the near-wellbore region of a reservoir. Pressure sensors were attached along the sandstone core and recorded the U-shaped pressure distribution generated during the transient experiments. Additionally, Obernkirchener Sandstone was selected as the core raw material for the experiments. However, the small rock sample size and relatively low injection pressure (5 barg) may have limited the laboratory evaluation to a certain degree, so a novel large-scale core-flooding experimental setup is designed and constructed in this study, allowing tests to be performed at a greater working pressure.

1.2 Core-flooding experiments

The properties of reservoir rock and fluid are universally investigated by the core-flooding experiments in the laboratory, where an elastic rubber sleeve that contains a core sample is placed in a cylindrical cavity with open ends (referred to as a core holder). The ends of the rubber sleeve are fitted over end plugs, where solid contacts are setup between the faces of end plugs and ends of the core sample. The open ends of the core holder can be sealed by end caps with O-rings. During a core-flooding experiment, the rubber sleeve will be compressed by the pressurized fluid in the annular space surrounding it to provide radial overburden pressure on the core sample. Axial overburden pressure can also be added, depending on the type of the core holder. The tested fluid is forced into one end of the core sample through the end plug with an inlet pressure/temperature and emerges at the other end of the core sample with an outlet pressure/temperature.

2. Review of existing core-flooding research facilities in the public domain

This section presents some selected core-flooding experimental setups from published laboratory studies, focusing on setup purpose, tested phases, core dimensions, core holder types, rock properties, produced fluids' separation and corresponding working conditions. This extended literature review is a preparation for the design of the core-flooding apparatus in this study.

Different porous media are chosen based on various experimental purposes, including sandstone, limestone, sand mixture and glass beads (Table 1). Most popular is sandstones due to its qualified permeability and porosity. In some cases, composite cores were applied in tests to obtain a core sample with larger dimensions (Alvarado et al., 2001). Large scale samples were only apparent in tests with unconsolidated artificial porous medium. The maximum length of sample was a test cell of 83.82 cm, packed with a mixture of sand, oil and water (Rivero and Mamora, 2005); the maximum length/diameter ratio was 18.13, using various diameter glass beads as artificial porous medium (Jamialahmadi et al., 2005).

Table 1 Review of existing core-flooding experimental setups in the public domain.

Related parameters	Ebeltoft et al., 1998	Darvish et al., 2006	Niz-Velasquez et al., 2009	Song and Renner, 2007	Aleidan and Mamora, 2010	Alvarado et al., 2001	Jamialahmadi et al., 2005	Rivero and Mamora, 2005	Konno et al., 2013	Shi, 2009
Setup purpose	Relative permeabilities measurements	CO_2 injection in fractured reservoirs	High pressure air injection	Analysis of oscillatory fluid flow	CO_2 flood study	Tracer dispersion	Pressure drop, gas hold-up and heat transfer through porous media	Steam-propane injection in heavy oil field	Permeability measurements in methane-hydrate-bearing sediments	Flow behaviour of gas-condensate wells
Involved phases	Three phase (synthetic formation water, white oil and nitrogen)	Two phase (CO_2 and oil)	Three phase (water, oil and gas)	Single phase (water)	Three phase (water, oil and CO_2)	Three phase (water, oil and gas)	Single/two phase (distilled water and air)	Three phase (water, oil, steam and propane gas)	Two phase (water and gas)	Two phase (butane, methane and water)
Porous medium	Berea sandstone	Chalk	Berea sandstone	Fontainebleau sandstone	Limestone	Composite core	Glass beads	Mixture of sand, oil and water	Toyoura standard sand	Berea sandstone
Permeability, mD	171.40	4	102.70 ± 2	0.1 - 1000	90	1390.50	4.62×10^4 – 1.72×10^6	-	25650	5
Porosity, %	19.5	44	-	5 -8	29	23.33	36.10 – 38.00	37.60 - 41.90	-	15
Diameter, cm	3.78	4.6	3.81	3	5.08	3.81	3.2	5.91	5	5.06
Length, cm	29.8	60	30.05	3 - 11	15.24	30	58	83.82	20	25.04
Length/Diameter	7.88	13.04	7.89	1.00 - 3.67	3	7.87	18.13	14.18	4	4.95
Inlet pressure, bar	-	300	176.71	40 - 50	131	110.32	-	4.03 - 5.29	82	134-138
Confining pressure, bar	50	-	-	200 - 1400	172	172.37	-	-	96	399
Confining pressure/Inlet pressure, bar	-	-	-	4.00	1.31	1.56	-	-	1.17	-
Temperature, °C	160 ± 0.1	130	80	-	48.89	113.33	20 -90	50	0.65	Room temperature
Flow rate, ml/min	-	0.10 - 5.6 (CO_2)	-	-	0.25-0.50 (CO_2); 0.25 (water)	0.20 (tracer)	1.92 – 336 (liquid); 0 – 14400 (gas)	~ 3.50 (injected water)	200 (gas); 0.1 (water)	-
Pressure Distribution Measurement	Not present	Not present	Not present	Not present	Not present	Not present	Available	Not present	Available	Available
Separator	Three-phase acoustic separator	Oil-gas separator	Liquid-gas separator	Not present	Liquid-gas separator	Not present	Liquid-gas separator	Two gas separators	Not present	Not present
Loop type	Close	Open	Open	Open	Open	Open	Open	Open	Open	Open
Core holder direction	Horizontal	Vertical	Horizontal	Vertical	Horizontal	Horizontal	Vertical	Vertical	Vertical	Horizontal
Experiment type	Steady-state/Unsteady-state	Steady-state	Steady-state	Transient	Steady-state	Steady-state	Steady-state	Unsteady-state	Steady-state	Steady-state

Differences between designed laboratory and actual reservoir conditions need to be compensated for. The inlet pressure of injected fluids was generally provided by fluids pumps or gas compressors; the largest being 300 bars (Darvish et al., 2006). Temperature was usually controlled via heating cables twined on the core holder. Alternatively, a temperature controllable compartment that could accommodate the entire holder was used; a maximum temperature of 160 °C was achieved for three-phase flow apparatus with an accuracy of ± 0.1 °C (Ebeltoft et al., 1998).

Few core-flooding experimental setups in Table 1 are capable of measuring pressure distribution along the core sample, as this type of measurement can only be realized by the specially made core holder with pressure taps molded. Also, laboratory tests tend to be under steady state or unsteady state conditions; very few involve time as a factor in their experiments.

3. Design and construction of the experimental apparatus

3.1 Core Sample Preparation

One of the essential objectives of this study was to upscale the previous small-scale core-flooding experiments carried out by Wang (2012) and Liu (2016). Thus, in order to ensure continuity in our experimental campaign, Obernkirchener Sandstone was used again as the core material in the large-scale tests presented here. Obernkirchener Sandstone is a consolidated, relatively fine grained, low permeability sedimentary rock produced from north Germany. Its components and properties are summarized in Table 2. As can be seen, more than 90% of this sandstone is made up of quartz, assuring its uniformed texture and compactness. In this study, a standard core plug drilled out of an Obernkirchener Sandstone block is used with a length of 80 cm and a diameter of 10.16 cm.

Table 2 Components and properties of Obernkirchener Sandstone (Wang, 2012).

Parameters	Values
Quartz, %	92
Feldspar, %	3.5
Rock Fragments, %	1.5
Opaque Minerals, %	0.75
Heavy Minerals, %	0.75
Clay Minerals, %	2
Median Pore Size, μm	15 ± 10
Porosity, %	15 - 20
Permeability, mD	5 - 20

3.2 Core holder

A hydrostatic “biaxial” type core holder was designed to accommodate a large-scale core plug of 80 cm in length and 10.16 cm in diameter, with an option to hold shorter core samples (Fig. 2). The core holder allows radial and axial confining pressures to be applied to the rock sample. Core Laboratories (USA) manufactured the core holder and its related accessories.

Fig. 2. Custom-made core holder for large-scale core-flooding experiments.

Fifteen pressure ports were molded along the length of the rubber sleeve (Fig. 3 a) and, to fully record the back pressure effects, more pressure ports were installed downstream of the system. The first pressure tap is 0.5 inch away from the right end surface, and the other nine pressure taps are evenly placed every inch along the length of the core. The tenth tap is mounted on the corresponding other side of the core plug because of space limitations. Another 5 ports are located upstream of the core holder every 4 inches. The taps and ports are connected with pressure-port tubing with a diameter of 1/16 inches (Fig. 3 b). Thus, dynamic pressure profiles could be recorded in detail along the rock sample during the transient period of tests.

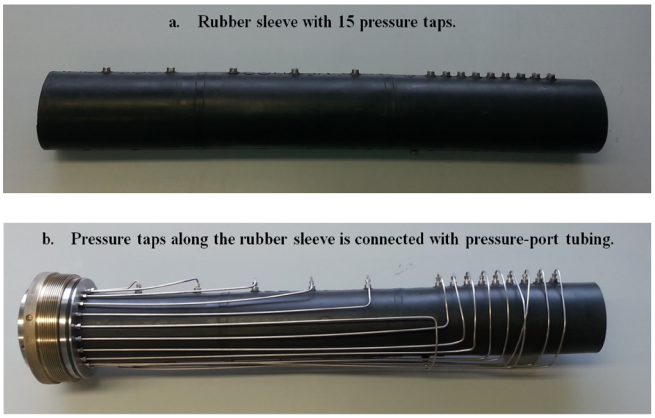

Fig. 3. Rubber sleeve with 15 pressure ports.

3.3 Description of the assembled experimental setup

The assembled experimental apparatus (Fig. 4) allows nitrogen from a gas cylinder to constantly flood the pressurized core plug placed in the hydrostatic core holder. Both radial and axial pressures are provided by a confining pressure pump to mimic overburden on the rock sample. The custom-made elastic rubber sleeve, molded with fifteen pressure taps, was placed in the core holder. For this study, only four taps were used, connected through pressure-port tubing to the fixed distribution plug, and linked to pressure sensors by steel tubing to measure transient pressure profiles along the core sample. Inlet and outlet pressures of the system were recorded by two extra pressure transducers on both ends of the core plug. The upstream and downstream pressures were controlled by the corresponding gas pressure regulators. During the tests, the opening position of the three-way valve determined whether the produced gas should go to either gas storage tank 1 or to gas storage tank 2 in order to manually induce pressure surges from downstream. The produced pressure waves at the outlet were employed to simulate the well/porous medium dynamical interface.

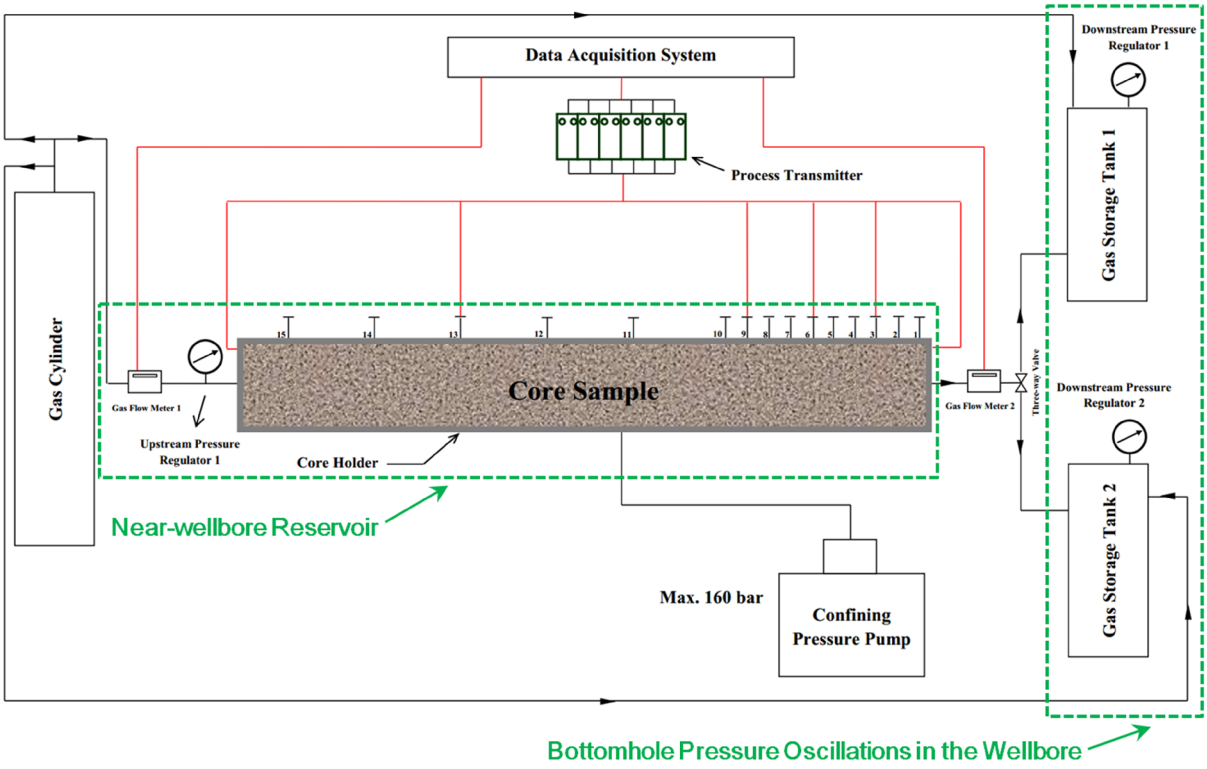

Fig. 4. Schematic of experimental setup for the large scale tests.

4. Comparison of major equipment against existing experimental setups

Compared to the conventional core-flooding experimental equipment described in the extensive literature review, this scaled up experimental setup consisted of four major improvements:

1. The customized hydrostatic core holder could accommodate one large-scale core sample of maximum length 80 cm and diameter 10.16 cm.
2. The dynamic pressure profile along the core sample could be accurately measured by the installed pressure taps distributed along the rubber sleeve.
3. The maximum working pressure for the test is up to 160 barg.
4. Both radial and axial confining pressures could be applied on the core plug.

The actual core size used in the large-scale experiments of this study (highlighted by the red dotted line frame in Fig. 5) was by far the largest in diameter and length.

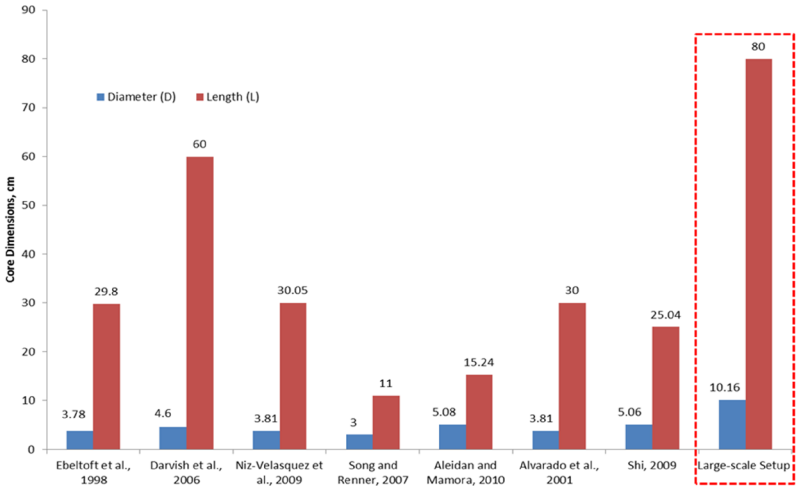

Fig. 5. Core dimensions of selected core-flooding experimental setups (only studies that used actual rock plugs are selected for this chart; the ones that used packed sand mixtures or glass beads into the core holder are excluded).

5. Experimental procedure

In this study, the test sequence consisted of three steps: permeability of the large-scale core sample was measured considering the Klinkenberg effect at low pressure conditions; experiments were then carried out at low pressure; the experiments were repeated, with relatively high inlet and outlet pressures imposed on the system to monitor the associated pressure distribution along the core sample during the transient period.

In the large-scale/low-pressure tests, two precision gas regulators were installed at the inlet and outlet of the experimental apparatus to ensure accurate pressure control up to 10 barg. Before each test, the tightness of the core holder was carefully checked to exclude any leakage. At the beginning of the test, the upstream and downstream pressures were defined as constant at 1 ~ 10 barg and 0 barg, respectively. When gas flow had stabilized under these conditions, the pressure at the outlet was increased (to 1 ~ 10 barg) by switching the three-way valve from the atmosphere to the gas storage tank connected to the downstream gas regulator.

In the large-scale/high-pressure tests, the inlet pressure was roughly regulated by a common industrial pressure reducer. Meanwhile, the outlet pressure was approximately controlled by an assembly of two relieve valves. The operating pressure of this setup was defined in the range of 10 ~ 50 barg. At the initial moment of the tests, both inlet and outlet pressures were regulated at a pressure greater than the atmospheric pressure (10 ~ 50 barg). Once the first steady state condition was reached, the downstream pressure was switched to a higher value (10 ~ 50 barg). The conversion of the two outlet pressures was still realized by the three-way valve connected to both gas storage tanks.

6. Discussion of experimental results

In what follows, the experimental results are presented through time histories of pressure distributions and flow rates during the transient periods.

6.1 Large-scale/low-pressure tests

U-shaped curves can be clearly observed in the pressure profiles recorded during the transient period of the large-scale/low-pressure test with an inlet pressure of 5 barg and an outlet pressure of 0/3 barg (Fig. 6). However, the development of the U-shaped pressure profiles is slower than expected. The delayed responses at the measuring point “a” are particularly obvious, suggesting location “a” felt the greatest influence from back pressure effects among the six pressure measurement points. During the experimental operation, the outlet pressure amplitude was manually controlled by the downstream three-way valve. Theoretically, the pressure value at point “a” should immediately increase from 0 barg to 3 barg at a time of 1s (t = 1s). In practice, the outlet pressure takes around 2s to reach the desired value. The monitored pressure at point “a” increases

from 0 barg to 3 barg at a time of 3s (t = 3s). This mismatch is due to the data acquisition system requiring 1 ~ 2s to respond to a pressure variation, yet the pressure transducers could only read the received signals after a rise time of 2 ~ 5 ms. To qualitatively display the obtained experimental data, error propagation analyses are included in Fig. 6, by means of error bars, to indicate the closeness of the measured to the true values.

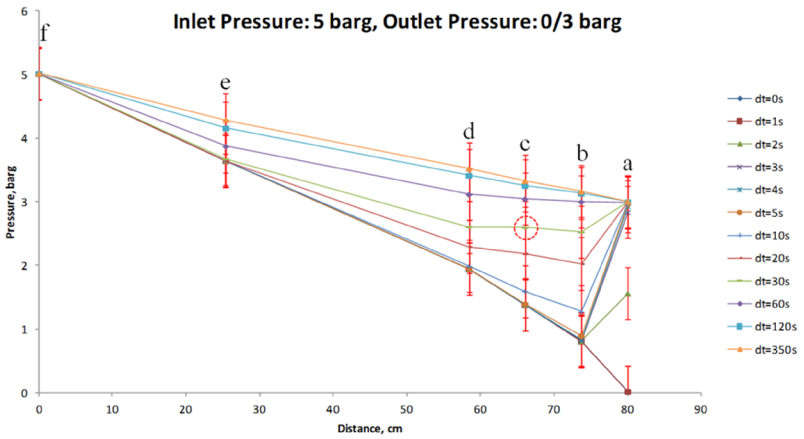

Fig. 6. Pressure profiles during transient period of the large-scale low-pressure experiments.

Upstream and downstream volumetric flow rates with an imposed outlet pressure of 0/3 barg were compared (Fig. 7). Upstream flow rate profiles decreased initially during the transient period, as a smaller pressure drop along the core sample was generated with the imposed outlet pressures, and then became flat as the second steady state condition was reached. Measurement gaps were observed in the downstream flow rate profiles at the beginning of transient periods, indicating the occurrence of counter flow at the outlet of the system, as the flow meters used could only monitor gas flow in one direction. This observed experimental phenomenon corresponds to the re-injection from the wellbore into the reservoir during liquid loading in gas wells. Later on, downstream flow rates flowed in the initial direction once more, indicating the end of counter flow. Finally, gas flowed steadily through the core plug at a lower flow rate than the initial state, indicating that the second steady state condition had been attained. The inlet and the outlet flow rates were nearly equal to each other under steady state conditions, as the volume flow rates displayed in all three cases were converted to standard pressure and temperature conditions adopted by the petroleum industry (18 °C and 1 bara).

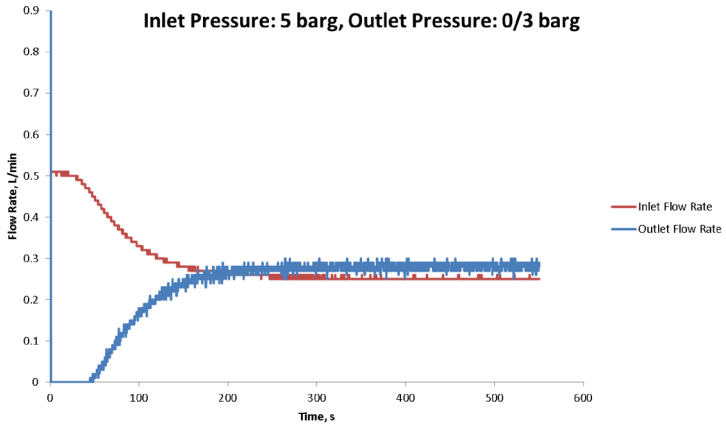

Fig. 7. Comparison of inlet and outlet flow rates during transient period of large-scale/low-pressure tests.

An unexpected feature other than the common "U-shaped" scenario, was observed in the experimental pressure data. The pressure value at measuring point "c" at a time of 30s (t = 30s), highlighted by the red dotted circle in Fig. 6, shows an unexpected pressure bulge, unlike the other pressure measurement points. The pressure bulge is attributed to a "pressure

shock" generated during the experiments. The theory of pressure shocks has been widely explored in gas dynamics (Gessner and Barbosa Jr., 2009). In the large-scale experiments shown here, the outlet pressure was suddenly increased from 0 to 3 barg at a time of 0s (t = 0s). During the start time period (0 ~ 3s), the outlet boundary pressure is higher than that in the core section very close to the outlet. Therefore, the gas at the outlet starts to flow in an opposite direction from the initial state, with limited gas mass entrance. This phenomenon is captured by the outlet flow meter's measurement gap at the beginning of the outlet flow rate profile (Fig. 7). At the same time, the inlet boundary, which is relatively far away from the outlet, still holds a constant pressure of 5 barg. Thus, the upstream gas flow is still flooding in the initial direction (from inlet to outlet). On the other hand, as a consequence of the sudden outlet pressure increase, more gas is injected from downstream over a relatively short time interval, while gas continues to come in steadily from upstream. This creates a pressure shock (i.e. the observed pressure bulge) at the measuring point c, where the gas flowing from upstream and that from downstream meet. The pressure shock is related due to fast mass accumulation/gas compression at the outlet.

6.2 Large-scale/high-pressure tests

The recorded pressure profiles during the transient period for an inlet pressure of 30 barg and an outlet pressure of 10/20 barg (Fig. 8) exhibit U-shaped pressure profiles, with a relatively short transient duration (within 20s). The pressure bulge that was observed in the low-pressure tests can still be observed in the high pressure cases, but is less severe. For example, the measuring point "c" (highlighted in the red dotted circle) suffered from the pressure shock during the development of U-shaped curves. Additionally, unexpected gas fluctuations are observed in the high-pressure tests. Normally, when the second steady state condition is reached, the outlet pressure should remain constant. However, the pressure at the measuring point "a" is still drifting within a relatively large range even after the U-shaped curves have disappeared (see the red double-headed arrow). This may have been caused by the current experimental limitations in the high-pressure tests. When the high-pressure experiments were carried out, the inlet pressure of the system was controlled by a pressure reducer located directly on the top of the gas bottle, and the corresponding outlet pressure was regulated by an assembly of gas storage tanks and relief valves. This design could not provide results as accurate as in the case of the low-pressure tests, where high-precision gas regulators could be used.

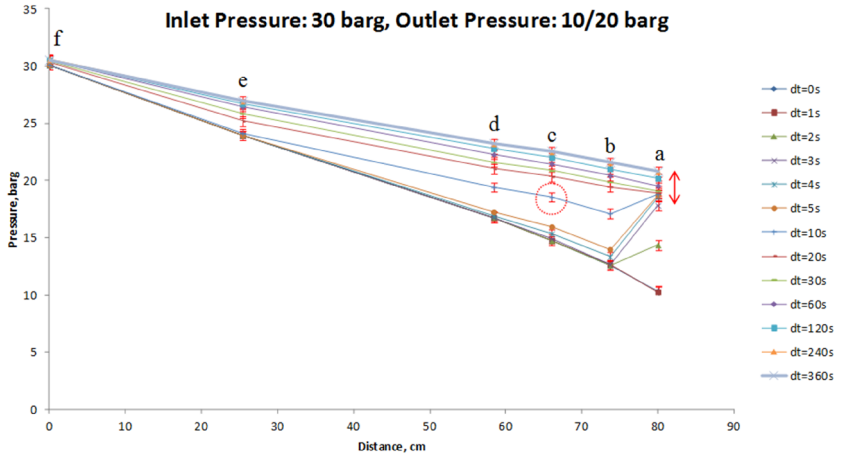

Fig. 8. Pressure profiles during transient period of the large-scale high-pressure experiments.

Comparisons of upstream and downstream flow rates for an inlet pressure of 30 barg and outlet pressures of 10/20 barg (Fig. 9) exhibit the same trends as the low-pressure tests. Inlet flow rates decline at the beginning of the transient period, while the outlet flow rate starts to increase from 0 L/min, yet finally, both profiles have nearly stabilized at constant flow rate values. As all volume flow rates were converted to 18 °C and 1 bara, the upstream and the downstream values should be equal, but gaps between them can be observed, most likely caused by gas fluctuations in the experimental system.

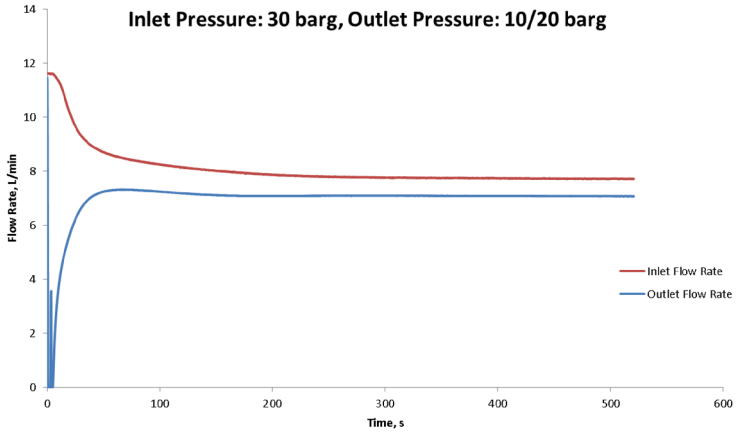

Fig. 9. Comparison of inlet and outlet flow rates during transient period of large-scale/high-pressure tests.

7. Conclusions and Recommendations

This study investigated the transient gas and gas-liquid flows in integrated reservoir/wellbore systems under liquid loading conditions. A novel large-scale core-flooding experimental setup was designed and custom-built to provide new insights into near-wellbore reservoir dynamic behaviors. One large-scale core sample, which was drilled out of an Obernkirchener Sandstone block, was tested in the experiments. The U-shaped pressure profile along the near-wellbore region of a reservoir under transient flow conditions, was experimentally reproduced for single-phase gas flow, and the U-shaped pressure distribution can be established during the dynamic interactions between wellbore and reservoir. The severity of these profiles largely depends on the magnitude of the downstream pressure oscillation, which directly influences the scale of the back pressure effects.

Unexpected pressure ‘bulges’ seen in the large-scale experiments were due to the outlet pressure being suddenly increased from atmospheric pressure to a relatively higher pressure. This led to gas being injected from downstream of the core sample over a relatively short time interval, with the gas continuing to come in steadily from upstream, resulting in a pressure shock when upstream and downstream gas flows met.

In order to better understand what is really happening in a liquid loaded well and the corresponding near wellbore region, further investigations will be required to run back pressure tests on different types of rocks.

References

Aleidan, A. and Mamora, D. D., SWACO2 and WACO2 Efficiency Improvement in Carbonate Cores by Lowering Water Salinity, SPE-137548-MS, Canadian Unconventional Resources and International Petroleum Conference, 19-21 October, Calgary, Alberta, Canada (2010)

Alvarado, V., Manrique, E., Ponce, R. and Lopez, P., Computer-Aided Analysis of Tracer Dispersion in Composite Cores: Tests of Two- and-Three Phase Flow Experiments, SPE-65374-MS, SPE International Symposium on Oilfield Chemistry, 13-16 February, Houston, Texas (2001)

Coleman, S.B., Clay, H.B., McCurdy, D.G., and Lee Norris, H. III, Understanding Gas-Well Load-Up Behavior, Journal of Petroleum Technology, Vol. 43, Issue 03, pp. 334-338 (1991)

Darvish, G.R., Lindeberg, E., Holt, T., Utne, S.A. and Kleppe, J., Reservoir Conditions Laboratory Experiments of CO2 Injection into Fractured Cores, SPE-99650-MS, SPE Europec/EAGE Annual Conference and Exhibition, 12-15 June, Vienna, Austria (2006)

Ebeltoft, E., Iversen, J.E., Vatne, K.O., Andersen, M.A. and Nordtvedt, J.E., A novel experimental apparatus for determination of three-phase relative permeabilities at reservoir conditions, Journal of Petroleum Science and Engineering, Vol. 19, Issues 1-2, pp. 119-132 (1998)

Falcone, G. and Barbosa Jr., J.R., State-of-the-art Review of Liquid Loading in Gas Wells, DGMK/ÖGEW-Frühjahrstagung 2013, Fachbereich Aufsuchung und Gewinnung Celle (2013)
Gessner, T.R. and Barbosa Jr., J.R., NUMERICAL ANALYSIS OF A TWO-PHASE SHOCK TUBE, 20th International Congress of Mechanical Engineering, November 15-20, Gramado, RS, Brazil (2009)

Jamialahmadi, M., Müller-Steinhagen, H. and Izadpanah, M.R., Pressure drop, gas hold-up and heat transfer during single and two-phase flow through porous media, International Journal of Heat and Fluid Flow, Vol. 26, Issue 01, pp. 156-172 (2005)

Konno, Y., Jin, Y., Uchiumi, T. and Nagao, J., Multiple-pressure-tapped core holder combined with X-ray computed tomography scanning for gas-water permeability measurements of methane-hydrate-bearing sediments, Review Scientific Instruments, Vol. 84, Issue 06 (2013)

Liu, X., Ph.D. thesis, Clausthal University of Technology, Clausthal-Zellerfeld, 2016.

Niz-Velasquez, E., Van Fraassen, K., Moore, R.G. and Mehta, S.A., An Experimental Study on Three-Phase Flow in High Pressure Air Injection (HPAI), Journal of Canadian Petroleum Technology, Vol. 48, Issue 09, pp. 47-53 (2009)

Rivero, J.A. and Mamora, D.D., Production Acceleration and Injectivity Enhancement Using Steam-Propane Injection for Hamaca Extra-Heavy Oil, Journal of Canadian Petroleum Technology, Vol. 44, Issue 02, pp. 50-57 (2005)

Shi, C., Ph.D. thesis, Stanford University, Stanford, 2009.

Song, I. and Renner J., Analysis of oscillatory fluid flow through rock samples, Geophysical Journal International, Vol. 170, Issue 1, pp. 195-204 (2007)

Wang, Y., Ph.D. thesis, Clausthal University of Technology, Clausthal-Zellerfeld, 2012.

Zhang, H., Falcone, G., and Teodoriu, C., Modelling Fully-Transient Two-phase Flow in the Near-Wellbore Region During Liquid Loading in Gas Wells, Journal of Natural Gas Science & Engineering, Vol. 2, Issue 2-3, pp. 122-131 (2010)